Composites Research

Vol. 34, No. 6, 373-379 (2021)
DOI: http://dx.doi.org/10.7234/composres.2021.34.6.373
ISSN 2288-2103(Print), ISSN 2288-2111(Online)

Special Issue Paper

Structural and Thermal Analysis and Membrane Characteristics of Phosphoric Acid-doped Polybenzimidazole/Strontium Titanate Composite Membranes for HT-PEMFC Applications

Kanakaraj Selvakumar*,, Ae Rhan Kim*,***†, Manimuthu Ramesh Prabhu**†, Dong Jin Yoo*,***†**

ABSTRACT: A series of novel PBI/$SrTiO_3$ nanocomposite membranes composed of polybenzimidazole (PBI) and strontium titanate ($SrTiO_3$) with a perovskite structure were fabricated with various concentrations of $SrTiO_3$ through a solution casting method. Various characterization techniques such as proton nuclear magnetic resonance, thermogravimetric analysis, atomic force microscopy (AFM) and AC impedance spectroscopy were used to investigate the chemical structure, thermal, phosphate absorption and morphological properties, and proton conductivity of the fabricated nanocomposite membranes. The optimized PBI/$SrTiO_3$-8 polymer nanocomposite membrane containing 8wt% of $SrTiO_3$ showed a higher proton conductivity of 7.95×10^{-2} S/cm at 160°C compared to other nanocomposite membranes. The PBI/$SrTiO_3$-8 composite membrane also showed higher thermal stability compared to pristine PBI. In addition, the roughness change of the polymer composite membrane was also investigated by AFM. Based on these results, nanocomposite membranes based on perovskite structures are expected to be considered as potential candidates for high-temperature PEM fuel cell applications.

Key Words: Polybenzimidazole, Perovskite structure, Nanocomposite membrane, Thermal stability

1. INTRODUCTION

Due to the recent rapid increase in industrial and domestic energy consumption and environmental pollution, researchers around the world are being required to develop renewable and sustainable energy storage and conversion technologies. Recently, sustainable energy conversion devices, including proton exchange membrane fuel cell (PEMFC), have attracted considerable attention in an electrical vehicle (EV), industrial plant, unmanned aerial vehicles (UAV_S), emergency backup power generation, and portable device applications due to their high efficiency, environmental friendliness, simplicity, quick startup, and low cost. Various investigations have been conducted in recent decades to optimize and develop PEMFC applications, along with the study of proton exchange membranes (PEMS) being particularly important [1-4]. At present, Nafion is used as a benchmark proton exchange membrane in fuel cell applications due to its chemical, thermal and mechanical stabilities along with high proton conductivity.

However, the Nafion and fluorinated polymers have high-cost, low conductivity, and low durability at high temperatures [5]. In recent decades, intensive efforts have been made to develop low-cost polymer-based membranes to replace Nafion in the fuel cell field. At present, organic-inorganic polymer nanocomposites have attracted considerable attention due to their improved physical, mechanical, thermal, and proton conductivity properties. These non-fluorinated membranes of poly(ether sulfone), poly(benzimidazole), poly(ether ether ketone), and poly(imide) are effectively used in PEM fuel cell application [6-9].

Received 17 December 2021, received in revised form 22 December 2021, accepted 22 December 2021

*Department of Life Science, Jeounbuk National University, Jeonju 54896, Korea
**Department of Physics, Alagappa University, Karaikudi 630004, India
***Department of Energy Storage/ Conversion Engineering (BK21 FOUR) of Graduate School, Jeounbuk National University, Jeonju 54896, Korea
†Corresponding authors: Dr. Ae Rhan Kim (E-mail: kimaerhan@jbnu.ac.kr), Dr. Manimuthu Ramesh Prabhu (E-mail: mkram83@gmail.com), and Prof. Dong Jin Yoo (E-mail: djyoo@jbnu.ac.kr)

Since inorganic nanofillers provide high thermal and mechanical stability and pristine polymers provide flexibility and multi-functional reactivity, the combination of inorganic nanoparticles and polymer membranes provide improved aforementioned properties and it could be used for high temperature (HT) PEMFCs [10-15].

Poly(benzimidazole) (PBI) is an aromatic heterocyclic polymer, which contains both proton acceptor (-N=) and proton donor (-NH-) hydrogen bonding sites in the polymer backbone that is an excellent candidate for use in HT-PEMFCs due to their excellent thermal and mechanical stability. Generally, PBI is a better electronic and ionic insulator, while doping with acid shows excellent proton conductivity properties. PBI doping with phosphoric acid (PA) is an interesting technique for HT-PEMFC applications due to its high boiling point temperature, non-volatile property, high thermal stability, and high proton conductivity [16,17]. On the other hand, PA molecules with amphoteric nature and high dielectric constant at low humidity are suitable properties for substituting H_2O molecules in HT-PEMFC, which can create hydrophilic channels for cation exchange in the PA doped PBI membranes.

Perovskite is a stable type of oxide with the general formula ABO_3 can be a suitable choice for this purpose. A (cation A is 12-coordinated by oxygen, has a large ionic radius, and has a size similar to that of an oxygen ion) and B (cation B is 6-coordinated by oxygen and has a small ionic radius located in the octahedral holes between the closed pack AO layers) are suitable cations for the perovskite structure in the ABO_3 formula of perovskite [18].

Perovskite structures obtained from transition elements such as Ba, Ra, and Sr can be used as hygroscopic materials to improve the humidity sensing performance [19]. The proton conduction mechanism of the materials when interacting with water is well known as cation conductors [20]. Studies on perovskite-type ABO_3 materials have improved in recent years owing to their high proton conductivity in a humid atmosphere at high temperatures (1000°C). The perovskite structures have high thermal, chemical, and mechanical stabilities. Perovskite-based $SrTiO_3$ displays a cubic structure with a lattice parameter of 3.91 Å and space group Pm3m [21]. In the regular octahedral coordination of the $SrTiO_3$ lattice, A-site occupies strontium cation, B-site occupies titanium, and oxide anion occupies periphery. It provides excellent proton transfer under certain atmospheric and doping conditions. Therefore, studies to improve the properties of cross-linked, composite or/and hybrid polymers are being conducted [22,23]. Among several types of PA-doped perovskites, such as PBI/Fe_2TiO_5 [24], PBI/$SrCeO_3$ [25], and PBI/$BaZrO_3$ [26], have been considered as potential materials to enhance the proton conductivity of composite membranes.

Based on the studies mentioned above, we designed PBI/$SrTiO_3$ nanocomposite membranes with different weight percentages of $SrTiO_3$ (2wt%, 4wt%, 6wt%, 8wt%, and 10wt%) and fabricated them by the solution casting method. In addition, through acid uptake, thermal stability, and proton conductivity tests of the fabricated polymer nanocomposite membranes, particularly the optimized PBI/$SrTiO_3$(8wt%) nanocomposite membrane, was evaluated to have improved thermal stability, proton conductivity, and surface roughness compared to other nanocomposites. We consider that the PBI/$SrTiO_3$ perovskite-based polymer nanocomposite membranes could be potential candidates for HT-PEMFC applications.

2. MATERIALS AND EXPERIMENTAL

2.1 Materials

3,3-Diaminobenzidine (DAB, 99%), phosphoric acid (PA, 85%, HPLC grade), titanium isopropoxide (99%), isophthalic acid (IPA, 99%), sodium bicarbonate ($NaHCO_3$, 99%), methanol (99%), strontium nitrate ($SrNO_3$, 99%), potassium hydroxide (KOH, 98%) were purchased from Sigma-Aldrich, India. Polyphosphoric acid (PPA, 85%), N,N-dimethylformamide (DMF, 85%), N,N-dimethylacetamide (DMAc, 85%), N-methyl-2-pyrrolidone (NMP, 85%), tetrahydrofuran (THF, 85%) were procured from Alfa-Aesar, India. Deionized (DI) water was used for all experimental procedure.

2.2 Preparation of PBI

The PBI was synthesized from DAB (4.32 g, 0.012 mmol), IPA (1.99 g, 0.012 mmol) in 150 mL of PPA as a condensing agent by the synthesis method of Scheme 1. That is, both DAB and IPA were added into a 300 mL two-necked flask equipped with a mechanical stirrer under a nitrogen (N_2) atmosphere. The mixture was then stirred at 220°C after 24 h, then an appropriate amount of DI water was added and neutralized with the aid of $NaHCO_3$. The obtained product was then washed with methanol and dried overnight in a vacuum oven at 120°C [27,28]. The molecular weight (M_W) of synthesized PBI was 75 kDa, which was calculated by Ubbelohde viscometric studies.

2.3 Synthesis of $SrTiO_3$

The synthesis of $SrTiO_3$ was carried out using a 1:1 stoichiometric ratio of metal cations of $SrNO_3$ and titanium (IV) isopropoxide. The metal cation precursors in the above ratio were separately dissolved in DI water to form a transparent homogeneous solution under constant stirring for 4 h. A similar mole % of KOH solution was then added to the metal cation solution to control the pH level. The resulting product was then heated in a tubular furnace at 1000°C in a N_2 atmosphere

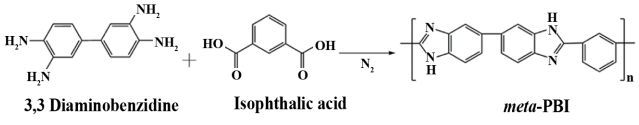

Scheme 1. Preparation of the PBI

for 6 h. The obtained samples were collected and various characterization techniques were applied.

2.4 Preparation of PBI/$SrTiO_3$–X composite membranes

As shown in Scheme 2, PBI/$SrTiO_3$-X nanocomposite membranes were prepared by the solution casting method. First, a proper amount of prepared PBI was dissolved in DMAc with stirring at 100~120°C. Thereafter, different weight percentages of $SrTiO_3$ (2wt%, 4wt%, 6wt%, 8wt%, and 10wt%) nanoparticles were added into the above PBI polymer solution, and the mixture was stirred at room temperature for 1 day. The obtained brown solution was poured into a Petri dish and kept at 160°C in an oven for 1 day. The resulting membranes were removed from the Petri dish and immersed in the PA solution. The obtained PBI/$SrTiO_3$-X (X is 2, 4, 6, 8, 10wt%) polymer composite membranes were stored in vacuum desiccators to avoid moisture absorptions. The thickness of the prepared polymer composites was measured at various positions using a digital screw gauge and thickness was about 50 μm.

2.5 Characterizations

Proton nuclear magnetic resonance (^{1}H NMR, JNM-ECA600-600 MHz) was used to ensure the chemical structure of the polymers using deuterated DMSO-d_6 as a solvent. The morphology and surface roughness of the pristine PBI and PBI/$SrTiO_3$ composite membranes were analyzed using an atomic force microscope (AFM, multimode 8, Bruker Corporation) in tapping mode. Thermogravimetric analysis (TGA) was performed using SDT Q600 systems. The TGA measurement was measured by heating from 25 to 1000°C under an N_2 atmosphere at a heating rate of 10°C/min.

2.6 Measurements

A piece of the composite membrane having a size of 1×1 cm was immersed in an 85% PA concentration solution for 1 day. The PA doping level of the membranes was defined as follows. The number of the PBI repeating units contained in 1 mole of PA is as shown in equation (1).

$$PA_{dop} = \left[\frac{\frac{w_1 - w_0}{98}}{\frac{w_0}{308}}\right] \quad (1)$$

Where w_o and w_1 are the weights of the dry membrane and doped membrane, respectively. Values 98 and 308 are the molecular weights of the PA and PBI repeat units, respectively. Leaching test is a method of measuring the residual amount of PA after washing the PA-doped PBI/$SrTiO_3$ nanocomposite membrane with hot water (the membrane is immersed in hot DI water at 90°C for 2 h). It is considered as one of the major decomposition factors of the PBI/$SrTiO_3$ composite membranes in fuel cells. AC impedance measurements were performed on polymer electrolytes using a computer-controlled μ-Auto lab Potentiostat/Galvanostat in the frequency range of 0.1 Hz to 10 MHz with a voltage amplitude of 50 mV [29]. Measurements were carried out in the potentiostat mode.

$$\sigma(S/cm) = L/RA \quad (2)$$

Where σ is the ionic conductivity value (S/cm), L is the thickness of the membrane film, R is the bulk resistance of the composite membrane film, and A (1 cm × 1 cm) is the area of the sample.

3. RESULTS AND DISCUSSION

3.1 NMR analysis of pure PBI

^{1}H NMR spectroscopy is used as a scrutinizing technique to confirm the presence of the polymer structure. The ^{1}H NMR spectrum of PBI with DMSO-d_6 solvent is shown in Fig. 1. The main peak 13.25 ppm is the amine protons of the benzimidazole moiety and peaks 7.59 to 9.15 ppm represent the aromatic groups of the polymer [28]. The results suggest that the carboxyl and amine groups are involved in the condensation process and copolymerization of IPA and DAB to PBI.

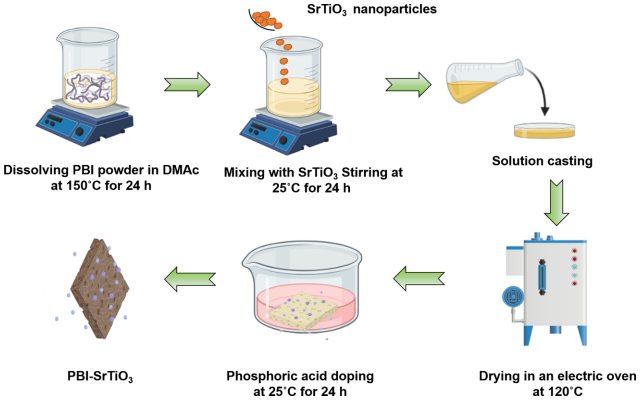

Scheme 2. Preparation of PBI/$SrTiO_3$–X composite membranes

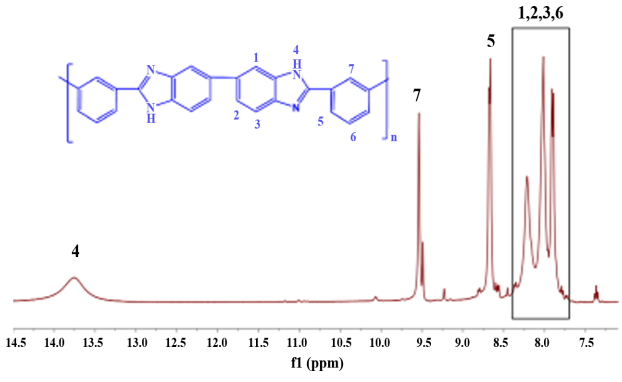

Fig. 1. ^{1}H NMR spectrum of the pristine PBI

3.2 PA doping, leaching, and solubility

PBI is a heterocyclic aromatic hydrocarbon polymer with a proton conductivity value of 1×10^{-4} S/cm. Therefore, the pristine PBI is not suitable for the PEM manufacturing process. After all, PA doping of PBI is necessary to improve proton conductivity. Moreover, PA act as a proton-conducting carrier, a hygroscopic compound, exhibiting proton conductivity in both anhydrous and hydrated states and does not require water for proton conduction in the composites [30]. Fig. 2 shows the PA uptake results of PBI and PBI/$SrTiO_3$ nanocomposite membranes. The incorporation of the perovskite $SrTiO_3$ nanoparticles with different wt% in the polymer electrolytes improved the ability to trap PA and thus enhanced the proton conductivity of the composite membranes. Therefore, all PBI/$SrTiO_3$ composite membranes showed high PA uptake and proton conductivity. Fig. 2 compares the acid doping percentage of pristine PBI and PBI/$SrTiO_3$-X (PBI < PBI/$SrTiO_3$-2 < PBI/$SrTiO_3$-4 < PBI/$SrTiO_3$-6 < PBI/$SrTiO_3$-8). However, the further addition of PBI along with $SrTiO_3$-10 markedly decreased the PA uptake value due to particle agglomeration and higher loading [31]. These results indicated that the amount of PA doping level is an important characteristic of proton conductivity.

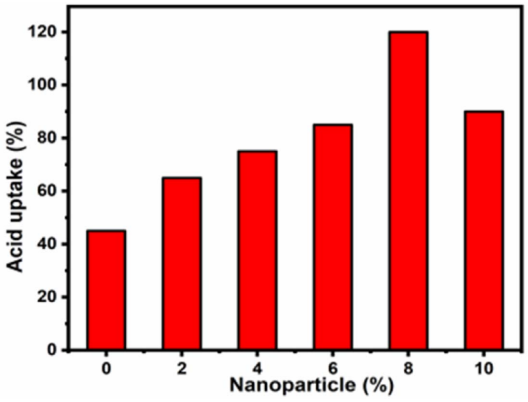

Fig. 2. Acid doping % plot for pristine PBI and composite polymer electrolytes

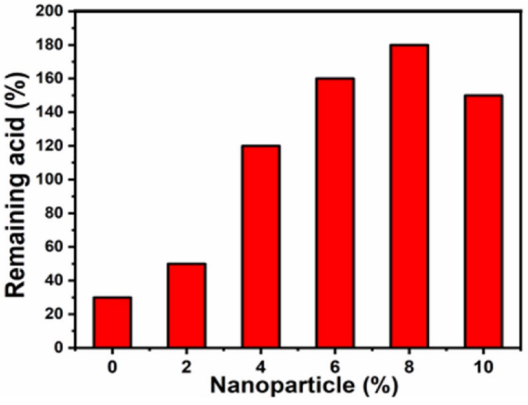

Fig. 3. The remaining acid % plot for pristine PBI and composite polymer electrolytes

The homogeneous and fine dispersion of nanoparticles in the polymer matrix increases the interface between the polymer and inorganic components even at high temperatures, effectively retaining the acid, thereby increasing the proton conductivity. The PA-doped polymer nanocomposite membranes were immersed in hot DI water for 3 h. The remained acids are related similarly to those described above. As shown in Fig. 3, the uniform homogeneous dispersion of $SrTiO_3$ in the polymer composites increases the interface between the proton-conducting polymer and perovskite nanoparticles even at high temperatures, which helps to effectively retain the acid and increase the proton conductivity [32]. The acid leaching test results in Fig. 3 show that the 8wt% $SrTiO_3$ membrane provides a high percentage of retention. Solubility is an initial checking process in the post-polymerization process. The pristine PBI (3 mg) was dissolved in 1 mL of various solvents such as THF, DMF, NMP, and DMAc. Yellow color transparent and flexible PBI and PBI/$SrTiO_3$ composite membranes were obtained from DMAc solvent.

3.3 Morphological study

Fig. 4 shows the 3 dimensional AFM images for pristine PBI and PBI/$SrTiO_3$-8 composite membrane. Fig. 4(A) shows the pristine PBI membrane has a uniform surface and no pores and defects observed in the image. It is due to the corresponding hydrophobic PBI matrix. Fig. 4(B) shows more roughness compared to pristine PBI. The average roughness (R_a) of the PBI/$SrTiO_3$-8 composite was calculated by AFM analysis, which indicates a quantitative idea of the difference in surface morphology. The R_a value of the PBI/$SrTiO_3$-8 composite membrane was found to be 25.13 nm. This indicates that the higher roughness of the PBI/$SrTiO_3$-8 composite membrane can enhance the uptake of PA molecules and the proton conductivity of the composite membrane because of its high surface area.

3.4 Thermal stability

Thermal stability of the composite membranes was performed using TGA analysis at a heating rate of 10°C/min in an N_2 atmosphere. The TGA curve of prepared composite membranes is shown in Fig. 5. It can be seen that the PA doped PBI/$SrTiO_3$-8 nanocomposite membrane exhibits high thermal stability compared to other nanocomposite membranes.

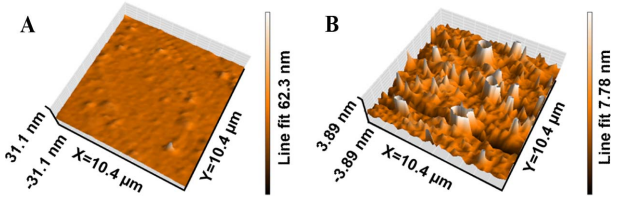

Fig. 4. AFM images for (A) Pristine PBI and (B) PBI/$SrTiO_3$-8

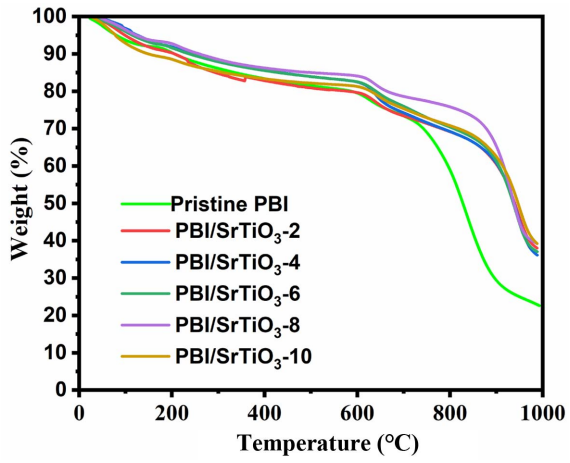

Fig. 5. TGA curves for (A) pristine PBI, (B) PBI/$SrTiO_3$-2, (C) PBI/$SrTiO_3$-4, (D) PBI/$SrTiO_3$-6, (E) PBI/$SrTiO_3$-8 and (F) PBI/$SrTiO_3$-10

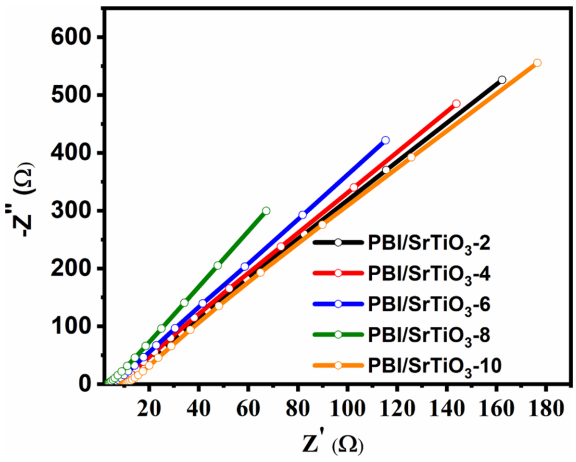

Fig. 6. Nyquist plot for PBI/$SrTiO_3$-2, PBI/$SrTiO_3$-4, PBI/$SrTiO_3$-6, PBI/$SrTiO_3$-8, and PBI/$SrTiO_3$-10 at 160°C

The initial weight loss between 100~150°C occurs due to the absorbed OH group molecules in the polymer composites [33]. The second weight-loss occurring at 160~200°C is owing to thermal changes in the PA to form pyrophosphoric and triphosporic acids as shown in below following equations [34].

$$2H_3PO_4 \rightarrow H_4P_2O_7 + H_2O \quad (3)$$

$$3H_4P_2O_7 \rightarrow 2H_5P_3O_{10} + H_2O \quad (4)$$

The third major weight loss that occurs at above 600°C is due to the main polymer degradation [35]. Since the incorporation of $SrTiO_3$ nanoparticles into the PBI polymer matrix increases the thermal stability of composite membrane, the obtained results explain that TGA shows high thermal properties of the PBI/$SrTiO_3$-8 nanocomposite membrane for HT-PEMFC.

3.5 AC impedance

The Nyquist plots of PA doped PBI with various concentrations of $SrTiO_3$ at 160°C are shown in Fig. 6. From Fig. 6, x-axis Z' is denoted as real part and the imaginary part is –Z" the bulk resistance R can be taken from intercept on the x-axis. Javan bakht *et al.* reported the proton conductivity of pristine PA-PBI was measured AC impedance method and the proton conductivity value of 5.12×10^{-3} S/cm at 160°C [25]. Proton conductivities were calculated from the bulk resistance of the composite membranes of Fig. 6 using equation (2). The maximum proton conductivity of the nanocomposite membrane was obtained at 7.95×10^{-2} S/cm at 160°C for the PBI/$SrTiO_3$-8 sample. It involves protons exchange between phosphoric acid, H_2PO^{4-} or HPO_4^{2-} and PBI. Additionally, strong acids can form polymeric complexes due to hydrogen bonding interactions or acid-base interactions between the imidazole group of PBI and the acid molecules from the oxygen to the nearest neighbor ion [36,37]. Moreover, the sites corresponding to the ABO_3 perovskite structure correspond to A-cation at the vertices of the unit cell, B-site cation in the center, and oxygen ion at the face of the cubic structure [38,39]. In particular, the cubic $SrTiO_3$ perovskite structure exhibits proton conductivity at high temperatures [40]. The proton conductivity of the nanocomposite increases with an increasing amount of $SrTiO_3$ nanofiller at 160°C. This enhancement of the proton conductivity of the PBI/$SrTiO_3$-8 sample is attributed to the hygroscopic properties of $SrTiO_3$ particles in the membrane. However, the conductivity value of the PBI/$SrTiO_3$-10 polymer composite membrane is decreased because some of the amino groups in PBI chains are blocked by $SrTiO_3$, which reduces the binding ability of the PBI chains to the PA groups.

4. CONCLUSIONS

The present study demonstrated the synthesis of PA doped PBI/$SrTiO_3$–X nanocomposite membranes and their characterization via NMR, physicochemical properties, TGA, AFM, and proton conductivity. The synergetic combination of the organic and inorganic phases of PBI/$SrTiO_3$ resulted in significant improvements. The highest PA uptake of 120% was observed for PBI/$SrTiO_3$-8 polymer electrolytes. TGA analysis revealed that these PBI nanocomposite membranes can stand temperatures of up to 200°C. The R_a value of the nanocomposite polymer electrolyte over the scanned area is around 25.13 nm. The highest proton conductivity was obtained at 7.95×10^{-2} S/cm at 160°C for PBI/$SrTiO_3$-8 polymer composite membrane. These results show that the acid absorption and proton conductivity of polymer composite membranes were higher than that of the pristine PBI membrane. These PBI/$SrTiO_3$ based composite membranes are promising membranes for high-temperature PEMFC applications.

ACKNOWLEDGMENT

This research was supported by Basic Science Research Program through the National Research Foundation of Korea (NRF) funded by the Ministry of Science, ICT and Future Planning (NRF-2020R1A2B5B01001458). This work was supported by grants from the Medical Research Center Program (NRF-2017R1A5A2015061) through the National Research Foundation (NRF), which is funded by the Korean government (MSIP).

REFERENCES

1. Hosseinabadi, P., Hooshyari, K., Javanbakht, M., and Enhessari, M., "Synthesis and Optimization of Nanocomposite Membranes Based on SPEEK and Perovskite Nanoparticles for Polymer Electrolyte Membrane Fuel Cell," *New Journal of Chemistry*, Vol. 43, 2019, pp. 16232-16245.
2. Vinoth Kannan, M., Kim, A.R., and Yoo, D.J., "Potential Carbon Nanomaterials as Additives for State-of-the-art Nafion Electrolyte in Proton Exchange Membrane Fuel Cells: A Concise Review," *RSC Advances*, Vol. 11, 2021, pp. 18351-18370.
3. Wei, Z., He, S., Liu, X., Qiao, J., Lin, J., and Zhang, L., "A Novel Environment-friendly Route to Prepare Exchange Membranes for Direct Methanol Fuel Cells," *Polymer Journal*, Vol. 54, 2013, pp. 1243-1250.
4. Kim, A.R., Vinoth Kannan, M., Lee, K.H., Chu, J.Y., and Yoo, D.J., "Enhanced Performance and Durability of Composite Membranes Containing Anatase Titanium Oxide for Fuel Cells Operating under Low Relative Humidity," *International Journal of Energy Research*, 2021, doi.org/10.1002/er.7477.
5. Uma, T., Suresh Kumar, K., Kishimoto, A., and Kimura, K., "Synthesis of Organic/inorganic Hybrid Composite Membranes and Their Structural and Properties," *Materials Letters,* Vol. 72, 2012, pp. 81-87.
6. Yoo, D.J., Hyun, S.H., Kim, A.R., Gnana Kumar, G., and Nahm, K.S., "Novel Sulfonated Poly(arylene biphenylsulfone ether) Copolymers Containing Bisphenylsulfonyl Biphenyl Moiety: Structural, Thermal, Electrochemical and Morphological Characteristics," *Polymer International,* Vol. 60, 2011, pp. 85-92.
7. Divya, K., Sri Abirami Saraswathi, M.S., Rana, D., Alwarappan, S., and Nagendran, A., "Custom-made Sulfonated Poly(ether sulfone) Nanocomposite Proton Exchange Membranes Using Exfoliated Molybdenum Disulfide Nanosheets for DMFC Applications," *Polymer Journal*, Vol. 147, 2018, pp. 48-55.
8. Sri Abirami Saraswathi, M.S., Rana, D., Nagendran, A., and Alwarappan, S., "Custom-made PEI/exfoliated-MoS_2 Nanocomposite Ultrafiltration Membranes for Separation of Bovine Serum Albumin and Humic Acid," *Materials Science and Engineering: C,* Vol. 83, 2018, pp. 108-114.
9. Han, D., and Yoo, D.J., "Mesoporous SiO_2 Mediated Polybenzimidazole Composite Membranes for HT-PEMFC Application," *Transactions of the Korean Hydrogen and New Energy Society,* Vol. 30, 2019, pp. 128-135.
10. Vinoth Kannan, M., Rama Krishnan, S., Kim, A.R., Lee, H.K., and Yoo, D.J., "Ceria Stabilized by Titanium Carbide as a Sustainable Filler in the Nafion Matrix Improves the Mechanical Integrity, Electrochemical Durability, and Hydrogen Impermeability of Proton-exchange Membrane Fuel Cells: Effects of the Filler Content," *ACS Applied Materials & Interfaces*, Vol. 12, 2020, pp. 5704-5716.
11. Javanbakht, M., Hooshyari, K., Enhessari, M., and Beydaghi, H., "Novel PVA/$La_2Ce_2O_7$ hybrid Nanocomposite Membranes for application in Proton Exchange Membrane Fuel Cells," *Iranian Journal of Hydrogen Fuel Cell,* Vol. 1, 2014, pp. 105-112.
12. Shabanikia, A., Javanbakht, M., Amoli, H.S., Hooshyari, K., and Enhessari, M., "Effect of $La_2Ce_2O_7$ on the Physicochemical Properties of Phosphoric Acid Doped Polybenzimidazole Nanocomposite Membranes for High-temperature Proton Exchange Membrane Fuel Cell," *Journal of the Electrochemical Society*, Vol. 161, 2014, pp. F1403-F1408.
13. Vinoth Kannan, M., Kim, A.R., Rama Krishnan, S., Yu, Y.T., and Yoo, D.J., "Advanced Nafion Nanocomposite Membrane Embedded with Unzipped and Functionalized Graphite Nanofibers for High-temperature Hydrogen-air Fuel Cell System: The Impact of Filler on Power Density, Chemical Durability and Hydrogen Permeability of Membrane," *Composites Part B: Engineering,* Vol. 215, 2021, pp. 108828-108843.
14. Gnana Kumar, G., Kim, A.R., Nahm, K.S., Yoo, D.J., and Elizabeth, R., "High Ion and Lower Molecular Transportation of the Poly Vinylidene Fluoride–hexa Fluoro Propylene Hybrid Membranes for the High Temperature and Lower Humidity Direct Methanol Fuel Cell Applications," *Journal of Power Sources,* Vol. 195, 2010, pp. 5922-5928.
15. Kim, A.R., Gabunada, J.C., and Yoo, D.J., "Amelioration in Physicochemical Properties and Single Cell Performance of Sulfonated Poly(ether ether ketone) Block Copolymer Composite Membrane Using Sulfonated Carbon Nanotubes for Intermediate Humidity Fuel Cells," *International Journal of Energy Research*, Vol. 43, 2019, pp. 2974-2989.
16. Stevens, J.R., Wieczorek, W., Randucha, D., and Jeffrey, K.R., "Proton Conducting Gel/H_3PO_4 Electrolytes," *Solid State Ionics*, Vol. 97, 1997, pp. 347-358.
17. Demirrors, A.F., and Inhofe, A., "$BaTiO_3$, $SrTiO_3$, $CaTiO_3$, and $Ba_xSr_{1-x}TiO_3$ Particles: A General Approach for Monodisperse Colloidal Perovskite," *Chemistry of Materials*, Vol. 21, 2009, pp. 3002-3007.
18. Enhessari, M., Kargar Razi, M., Etemad, L., Parviz, A., and Sakhae, M., "Structural, Optical and Magnetic Properties of the Fe_2TiO_5 Nanopowders," *Journal of Experimental Nanoscience*, Vol. 9, 2011, pp. 167-176.
19. Phair, J.W., and Badwal, S.P.S., "Review of Proton Conductors for Hydrogen Separation," *Ionics*, Vol. 12, 2006, pp. 103-115.
20. Raja, K., Raja Pugalenthi, M., and Ramesh Prabhu, M., "Investigation on SPEEK/PAI/$SrTiO_3$-based Nanocomposite Membrane for High-temperature Proton Exchange Membrane Fuel Cells," *Ionics*, Vol. 25, 2019, pp. 5177-5188.
21. Troy, T.K., Browning, N.D., and Osterloh, F.E., "Nanoscale Strontium Titanate Photocatalyst for Overall Water Splitting,"

ACS Nano, Vol. 6, 2012, pp. 7420-7426.

22. Faharani, H., Wagiran, R., and Hamidon, M.N., "Humidity Sensors Principle, Mechanism, Fabrication Technologies: A Comprehensive Review," *Sensors*, Vol. 14, 2014, pp. 7881-7939.
23. Hooshyari, K., Heydari, S., Javanbakht, M., Beydaghi, H., and Enhessari, M., "Fabrication and Performance Evaluation of New Nanocomposite Membranes Based on Sulfonated Poly(phthalazinone ether ketone) for PEM Fuel Cells," *RSC Advances,* Vol. 10, 2020, pp. 2709-2721.
24. Shabanikia, A., Javanbakht, M., Amoli, H.S., and Enhessari, M., "Novel Nanocomposite Membranes Based on Polybenzimidazole and Fe_2TiO_5 Nanoparticles for Proton Exchange Membrane Fuel Cells," *Ionics*, Vol. 21, 2015, pp. 2227-2236.
25. Shabanikia, A., Javanbakht, M., Amoli, H.S., Hooshyari, K., and Enhessari, M., "Polybenzimidazole, Strontium Cerate Nanocomposites with Enhanced Proton Conductivity for Proton Exchange Membrane Fuel Cells Operating at High Temperature," *Electrochimica Acta*, Vol. 154, 2015, pp. 370-378.
26. Hooshyari, K., Javanbakht, M., Shabanikia, A., and Enhessari, M., "Fabrication $BaZrO_3$/PBI Based Nanocomposite as a New Proton Conducting Membrane for High-temperature Proton Exchange Membrane Fuel Cells," *Journal of Power Sources*, Vol. 276, 2015, pp. 62-72.
27. Arunbabu, D., Sannigrahi, A., and Jana, T., "Blends of Polybenzimidazole and Poly Vinylidene Fluoride for Use in Fuel Cell", *The Journal of Physical Chemistry B*, Vol. 112, 2008, pp. 5305-5310.
28. Selvakumar, K., and Ramesh Prabhu, M., "Enhancing Proton Poly(benzimidazole) with Sulfonated Titania Nanocomposite Membrane for PEM Fuel Cell Applications," *Macromolecular Research,* Vol. 29, 2021, pp. 111-119.
29. Matrina, P., Gayathiri, R., Raja Pugalenthi, M., Cao, G., Liu, C., and Ramesh Prabhu, M., "Nano Sulfonated Silica Incorporated SPEEK/SPVdF-HFP Polymer Blend Membrane for PEM Fuel Cell Application," *Ionics*, Vol. 26, 2020, pp. 3447-3458.
30. Ryu, S.K., Vinoth Kannan, M., Kim, A.R., and Yoo, D.J., "Effect of type And Stoichiometry of Fuels on the Performance of Polybenzimidazole-based Proton Exchange Membrane Fuel Cells Operating at the Temperature Range of 120-160°C," *Energy*, Vol. 238, 2022, pp. 121791-121795.
31. Yamazaki, Y., Jang, M.Y., and Taniyama, T., "Proton Conductivity of Zirconium Tricarboxybutylphosphonate/PBI Nano Composite Membrane," *Science and Technology of Advanced Materials*, Vol. 5, 2004, pp. 455-459.
32. Kawahara, M., Morita, J., Rikukawa, M., and Ogata, N., "Synthesis and Proton Conductivity of Thermally Stable Polymer Electrolyte: Poly(benzimidazole) Complexes with Strong Acid Molecules," *Electrochimica Acta*, Vol. 45, 2000, pp. 1395-1398.
33. Kim, A.R., and Yoo, D.J., "A Comparative Study on Physiochemical, Thermomechanical, and Electrochemical Properties of Sulfonated Poly(ether ether ketone) Block Copolymer Membranes with and without Fe_3O_4 Nanoparticles," *Polymers,* Vol. 11, 2019, pp. 536-551.
34. Artimani, J.S., Ardjmand, M., Enhessari, M., and Javanbakht, M., "Polybenzimidazole/$BaCe_{0.85}Y_{0.15}O_{3-\delta}$ Nanocomposites with Enhanced Proton Conductivity for High-temperature PEMFC Application," *Canadian Journal of Chemistry*, Vol. 97, 2019, pp. 1-21.
35. Kudakova, V., Quartarone, E., Mustarelli, P., Mangistris, A., Caponetti, E., and Saladino, M.L., "PBI-based Composite Membranes for Polymer Fuel Cells," *Journal of Power Sources*, Vol. 195, 2010, pp. 7765-7769.
36. Onitshi, T., and Helgaker, T., "A Theoretical Study on Hydrogen Transport Mechanism in $SrTiO_3$ Perovskite," *International Journal of Quantum Chemistry*, Vol. 112, 2012, pp. 201-207.
37. Tanaka, R., Yamamoto, H., Kawamura, S., and Iswase, T., "Proton Conducting Behavior of Poly(ethylenimine)-H_3PO_4 Systems," *Electrochimica Acta*, Vol. 40, 1995, pp. 2421-2424.
38. Shin, S., Huang, H.H., Ishigame, M., and Iwahara, H., "Proton Conduction in the Single Crystals $SrZrO_3$ and $SrCeO_3$ Doped with Y_2O_3," *Solid State Ionics*, Vol. 40-41, 1990, pp. 910-913.
39. Muthuraja, P., Prakash, S., Shanmugam, V.M., Radhakrsihnan, S., and Manisankar, P., "Novel Perovskite Structured Calcium Titanate-PBI Composite Membranes for High-temperature PEM Fuel Cells: Synthesis and Characterizations," *International Journal of Hydrogen Energy*, Vol. 43, 2018, pp. 4763-4772.
40. Kreuer, K.D., "Proton-conducting Oxides," *Annual Review of Materials Research,* Vol. 33, 2003, pp. 333–359.